Commun Nonlinear Sci Numer Simulat 90 (2020) 105403

Contents lists available at ScienceDirect

Commun Nonlinear Sci Numer Simulat

journal homepage: www.elsevier.com/locate/cnsns

Research paper

Impact of inter-layer hopping on epidemic spreading in a multilayer network

Dayu Wu[a,b], Ming Tang[a,b,*], Zonghua Liu[a], Ying-Cheng Lai[c]

[a] School of Physics and Electronic Science, East China Normal University, Shanghai 200241, China
[b] Shanghai Key Laboratory of Multidimensional Information Processing, East China Normal University, Shanghai 200241, China
[c] School of Electrical, Computer and Energy Engineering, Arizona State University, Tempe, AZ 85287, USA

ARTICLE INFO

Article history:
Received 28 February 2020
Revised 31 May 2020
Accepted 9 June 2020
Available online 12 June 2020

Keywords:
Multiplex network
Inter-layer hopping
Epidemic spreading
Quenched mean-field

ABSTRACT

Hopping of individuals among distinct layers can induce inter-layer coupling and consequently affect the spreading process in each layer of real world multilayer networks. We articulate a two-layer network model where a fraction of nodes are inter-layer travelers that can hop between layers. We develop a theoretical framework based on the quenched mean-field approximation to accurately predict the epidemic thresholds and final states in both layers. Extensive numerical simulations on synthetic and empirical networks demonstrate that, in the general setting where the structures of the two network layers are asymmetric, intense hopping can lead to simultaneous epidemic outbreak in both layers. In general, the impacts of hopping on the spreading dynamics in the two layers can be quite distinct. As the inter-layer coupling strength is increased, the epidemic threshold of the denser layer increases monotonically, while for the sparser layer, a surprising non-monotonic behavior of the threshold with a minimize value arises. Another finding is that, as a result of hopping, recurrent outbreaks can occur in the sparser layer, providing a plausible explanation for the phenomenon of multiple outbreaks observed from real health data.

1. Introduction

Dynamical processes on complex networks [1] constitute a main area of research in network science because of their relevance not only to science and engineering, but also to a host of problems in broader contexts such as sociology, economics, and political science. Among the commonly studied processes, epidemic spreading is fundamental to health care, social, economical, and political activities as well as information technologies [2,3]. The rapid spread of a novel coronavirus (COVID-19) creates great attention to the researches on disease prevention and control [4]. Generally, disease or virus spreading is not an isolated process that occurs in a single network, but rather, the dynamics are also affected by behaviors in other interdependent systems, such as a communication network (or layer) in which information about the disease propagates and gets exchanged. The dynamics in the communication layer can then raise some individuals' awareness about the disease, prompting them to take preventive measures. As a result, the epidemic threshold would be modified and a large-scale outbreak may be suppressed. A comprehensive, realistic and accurate description of the epidemic spreading dynamics thus requires a modeling framework based on multiplex or multilayer networks [5–8].

* Corresponding author at: School of Physics and Electronic Science, East China Normal University, Shanghai 200241, China.
E-mail address: mtang@ce.ecnu.edu.cn (M. Tang).

https://doi.org/10.1016/j.cnsns.2020.105403
1007-5704/

In general, there are two types of multilayer networks [9]: interconnected networks and multiplex networks. In an interconnected system, some of the nodes from the various subnetworks are adjacent to each other, so that the network effectively constitutes a single layer with interconnected communities [5]. In a multiplex network, a fixed set of nodes are connected by different types of links in different layers. That is, each node in a layer has its counterpart in the other layers coupled by one-to-one interconnections and each layer has a distinct internal connecting structure [9]. The characteristic feature that distinguishes a multilayer system from a single layer network is the interaction or coupling among the distinct layers. Previous studies revealed that inter-layer coupling can have a significant effect on network dynamical processes such as percolation [10], epidemic spreading [11], cascading failures [12], and diffusion process [13]. For example, for epidemic spreading, disease or virus can be transmitted with some probability through interconnections between the subnetworks or layers, which can promote spreading [14]. In particular, if the interconnections are strong, epidemics can occur simultaneously across the entire system [15], but if the layers are only weakly interconnected, spreading would be limited to a single or a few layers only [11]. For diffusion process, the multiplex structure can speed up the less diffusive of the layers because of the super-diffusion process between the layers of multiplex networks [16]. For reaction-diffusion system, patterns formation in multiplex networks was studied by means of a developed perturbative approach, and the interaction between layers can yield self-organized patterns [17]. The spreading dynamics of multiple viruses on multilayer networks have also been studied [6,18].

In previous studies, a common approach to modeling the interactions among the multiple network layers was to assume a fixed, time-independent transmission rate for the inter-layer connections. While this facilitates analysis of the spreading dynamics, there are situations in the real world where this assumption fails to describe. For example, in a two-layer model for spreading between two coupled subpopulations, the interaction between the two layers are result of human dynamics, for which a description based on a fixed transmission rate is inadequate [19]. In transportation networks, passengers tend to travel along the fastest paths connecting two stations by switching or hopping between, e.g., a bus network and a subway network [20]. The hopping behavior is also common in multiplex social networks, where an individual switches from one kind of interaction to another [21]. For instance, an individual first rings up one of his/her friends in the communication layer and then meets with the friend in the physical contact layer. To our knowledge, the question of how hopping among network layers affects the spreading dynamics on multiplex systems has not been addressed previously.

In this paper, we incorporate inter-layer hopping or traveling into multilayer network systems to investigate the impacts of the network layer hopping behavior on spreading dynamics. We develop an analytic theory to predict the key quantities characterizing the spreading dynamics such as the epidemic threshold, and provide extensive numerical support. Our main findings are the following. The first result is somewhat expected: for sufficiently large values of the hopping strength, simultaneous outbreak of the disease in both layers (i.e., denser and sparser layers) can occur. The second result is that the epidemic thresholds for the denser and sparser layers display distinct dependence on inter-layer hopping. Thirdly, the sparser layer can exhibit multiple (resurgent) epidemic outbreaks, a phenomenon that has been observed from empirical data of infectious diseases. The ability for the hopping to influence epidemic dynamics in a sensitive manner as revealed in our work suggests that the activities can potentially be exploited for controlling virus or information outbreaks in multilayer networks with significant applications in e.g., social, economical, political, and computer systems.

2. Multilayer network model with inter-layer hopping and quenched mean-field approach

2.1. Model

To accommodate inter-layer hopping, we stipulate that the two-layer system hosts two kinds of nodes: permanent "residents" and inter-layer travelers, where the former are "confined" to one network layer and the latter can switch or hop from one layer to another and vice versa. A permanent resident has fixed and stable connections only in one network layer, and his/her social relationship with nodes in the other network layer is non-existent or negligible, but a traveler has relatively stable social relationships in both layers. When a traveler is active in layer A, he/she is in contact with his/her neighbors in layer A. As the traveler switches to layer B, his/her connections in layer B are activated, leaving his/her connections in layer A dormant so that the links cannot transmit or receive the disease.

To characterize the interaction or coupling between the two layers, we introduce two layer-hopping parameters: the fraction m and activity level q of the inter-layer travelers. Especially, if layers A and B have the same network size N, the number of inter-layer travelers will be mN. When a traveler is in layer A (or B), he/she switches to his/her counterpart in layer B (or A) at the rate q_B (or q_A). A schematic illustration of the two-layer network model is shown in Fig. 1. In the steady state, the expected numbers of travelers in layers A and B are $\langle M_A\rangle = (mq_AN)/(q_A+q_B)$ and $\langle M_B\rangle = (mq_BN)/(q_A+q_B)$, respectively. For simplicity, we set $q_A = q_B = q$. The expected numbers of inter-layer travelers and permanent residents in layer A or B are $\langle M_A\rangle = \langle M_B\rangle = mN/2$ and $N_A^{'} = N_B^{'} = (1-m)N$, respectively. The double layer network model is appropriate for describing some real-life scenarios, particularly social networks (e.g., two interconnected city networks, Facebook and Twitter, WeChat and QQ, etc.).

To investigate the impacts of inter-layer hopping on epidemic spreading dynamics, we implement the classical susceptible-infected-recovery (SIR) process on the two-layer network model. In the SIR model [2,22–27], there are three possible states of a node: susceptible (S), infected (I), and recovered or refractory (R). If an S-state node contacts an I-state neighbor, the rate of the node being infected is β (the infection rate). Nodes in the infected state are recovered with rate

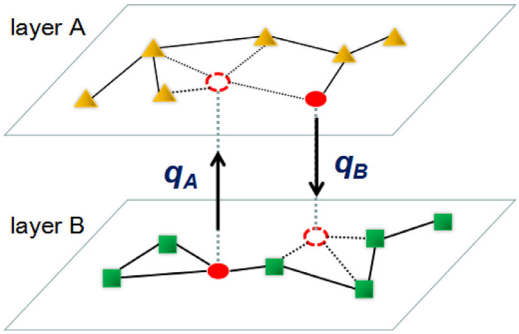

Fig. 1. Schematic illustration of two-layer network model with inter-layer hopping. The networks are composed of four types of nodes: permanent residents in layer A (orange triangles), permanent residents in layer B (green squares), inter-layer travelers (red solid circles) and the cavities left behind (red open circles). A traveler has corresponding nodal positions in layers A and B. When the traveler is in layer A, his/her corresponding node in layer B is in a hole state. During his/her stay in layer A, the traveler does not interact with any neighbor in layer B: his/her inner-layer edges there are dormant. When the traveler is active in layer A (B), the rate of switching to layer B (A) is q_B (q_A). (For interpretation of the references to color in this figure legend, the reader is referred to the web version of this article.)

μ. When there is no infected node in the network, i.e., all the infected nodes turn into the recovered state, the spreading process reaches a final state. At the end of the spreading, the outbreak size of epidemic is defined as the number of the recovered nodes. If the infection rate β is greater than an epidemic threshold β_c, a global epidemic outbreak with a finite fraction of outbreak size will emerge.

2.2. Quenched mean-field approach

We develop a theory to understand and predict the impacts of inter-layer hopping on epidemic spreading based on the framework of the quenched mean-field approximation (QMF). The QMF is an individual-based mean-field theory, where the probability of each individual being in the infected state is expressed [2,3]. Let $X_i(t) \in \{0, 1, 2\}$ be a variable denoting that, at time t, node i is in the susceptible, infected, and recovered state, respectively. The probabilities of node i being in the S, I, R states at time t can be denoted as $s_i(t) = G[X_i(t) = 0]$, $\rho_i(t) = G[X_i(t) = 1]$, and $r_i(t) = G[X_i(t) = 2]$, respectively, where G is a general probability function of the nodal state.

A multilayer network can be represented as a supra-adjacency matrix [9]. When there are no interconnections between layers A and B, the adjacency matrix of the system [with size $(N_A + N_B) \times (N_A + N_B)$] is given by

$$G_C = \begin{bmatrix} G_A & 0 \\ 0 & G_B \end{bmatrix}, \tag{1}$$

where G_A and G_B are the adjacency matrices of layers A and B when isolated, respectively. When there are inter-layer travelers, the hopping generates interconnections between the layers. If there is an interconnection between node i in layer A and node j in layer B, both nodes correspond to the same traveler. From node i (or node j), the traveler can switch to the counterpart node j (or node i) at the hopping rate q. The hopping behavior of the inter-layer travelers is actually a diffusion process. We can thus define an inter-layer connection matrix G_H of size $(N_A + N_B) \times (N_A + N_B)$. For a pair of nodes i and j at which the traveler is present or absent in the respective layers, the four matrix elements are $h_{ii} = -1$, $h_{jj} = -1$, $h_{ij} = 1$, and $h_{ji} = 1$, while other matrix elements in the ith and jth rows/columns are zero. Considering that the inter-layer hopping rate is $q_A = q_B = q$, the inter-layer diffusion process can be represented as a inter-layer Laplacian matrix $\mathcal{L}_H = qG_H$ with the property of any zero-sum row [16,17].

For SIR spreading, the time evolution equations of the two-layer network system, when inter-layer hopping is taken into account, are[28]

$$\frac{ds_i(t)}{dt} = -s_i(t)[1 - \prod_{j=1}^{N_A+N_B}(1 - \beta c_{ij}\rho_j(t))] + q\sum_{j=1}^{N_A+N_B} h_{ij}s_j(t), \tag{2}$$

$$\frac{d\rho_i(t)}{dt} = s_i(t)[1 - \prod_{j=1}^{N_A+N_B}(1 - \beta c_{ij}\rho_j(t))] + q\sum_{j=1}^{N_A+N_B} h_{ij}\rho_j(t) - \mu\rho_i(t), \tag{3}$$

$$\frac{dr_i(t)}{dt} = \mu\rho_i(t) + q\sum_{j=1}^{N_A+N_B} h_{ij}r_j(t), \tag{4}$$

where the first term on the right hand side of Eq. (2) is the probability that node i becomes infected by its neighbors at time t, the second term represents the influence of inter-layer traveler on the probability of node i being in the S state.

For the probability of node i being in the I state, the first term on the right hand side of Eq. (3) has the same form with Eq. (2) but opposite sign, the second term represents the influence of inter-layer traveler on the infected density, and the last term represents the probability of node i to have been recovered at time t. The first term on the right hand side of Eq. (4) has the same form with the last term of Eq. (3), and its second term represents the influence of inter-layer traveler on the recovered density.

For deducing the threshold, we linearize the above expression by considering that the fraction of infected people is very small at critical point: $\rho_i(t) = \epsilon_i(t) \ll 1 \forall i \forall t$ [29]. So that we can neglect the second-order terms in $\epsilon_i(t)$ in Eq. (3). A permanent resident stays only at some node of one layer, and its probability in the susceptible state at the critical point of theshold value is $s_i(t) = 1 \forall i \forall t$. The linearized form of Eq. (3) is

$$\frac{d\rho_i(t)}{dt} = \beta \sum_{j=1}^{N_A+N_B} c_{ij}\rho_j(t) - \mu\rho_i(t) + q \sum_{j=1}^{N_A+N_B} h_{ij}\rho_j(t). \tag{5}$$

An inter-layer traveler has the probability of 1/2 (i.e., $q_A/(q_A+q_B)$ and $q_A = q_B = q$) to be located at node i in layer A or at the counterpart node j in layer B. The probabilities of nodes i and j being in the susceptible state at critical point of threshold value can then be set to be 0.5. The linearized form of Eq. (3) for inter-layer travelers is

$$\frac{d\rho_i(t)}{dt} = \beta \sum_{j=1}^{N_A+N_B} 0.5c_{ij}\rho_j(t) - \mu\rho_i(t) + q \sum_{j=1}^{N_A+N_B} h_{ij}\rho_j(t). \tag{6}$$

Eqs. (5) and (6) can be combined into a convenient matrix form

$$\frac{d\vec{\rho}(t)}{dt} = (\beta G_D + qG_H - \mu E)\vec{\rho}(t), \tag{7}$$

where E denotes the identity matrix, $\vec{\rho} = [\rho_1(t), \rho_2(t), \cdots, \rho_{N_A+N_B}(t)]^T$. The two corresponding nodes of an inter-layer traveler have elements $d_{ik} = 0.5c_{ik}$ $(k = 1, 2, \ldots, N_A)$ for layer A and $d_{jk} = 0.5c_{jk}$ $(k = N_A+1, \ldots, N_A+N_B)$ for layer B in the matrix G_D, respectively, and the other elements are the same as that of G_C. The inter-layer Laplacian matrix qG_H is used to describe the inter-layer diffusion process. Eq. (7) illustrates one of the key concepts in the classical theoretical analysis of epidemic models.

The system enters a global epidemic region in which the epidemic grows exponentially when the largest eigenvalue of the matrix $\beta G_D + qG_H - \mu E$ is greater than zero [2]. That is, the outbreak size grows exponentially with time. Thus, we can obtain the epidemic threshold β_c by solving

$$\beta = \frac{\mu}{\Lambda_M(\beta)}, \tag{8}$$

and $\Lambda_M(\beta)$ is the largest eigenvalue of the matrix [29,30]

$$G_M(\beta) = G_D + \frac{\mathcal{L}_H}{\beta}, \tag{9}$$

where the supra-adjacency matrix G_D contains the intra-layer connection information and the inter-layer Laplacian matrix $\mathcal{L}_H$ (i.e., qG_H) represents the diffusion process between layers [16,17]. If the infection rate β is greater than the epidemic threshold β_c, a global epidemic outbreak will emerge.

3. Results

The simulation setting is as follows. The hopping induced interactions between the two network layers can be conveniently characterized by the fraction m and the hopping rate q of inter-layer travelers. We focus on how variations in these parameters affect the epidemic threshold and the outbreak size. To be concrete, we assume that both layers have the same network size ($N_A = N_B \equiv N$). The simulation experiments are implemented in synchronous updating method with discrete time steps, we set the time interval of each time step as $\delta t = 1$, and thus the probability of disease transmission through one link is equal to the infection rate β and the recovery probability of an infected node is μ in each time step [31]. We run our experiments on the Erdös-Rényi networks first, and then verify our conclusion on heterogeneous synthetic and empirical networks. The number of pairs of nodes with a one-to-one interconnection between the two layers is mN. The dynamical processes in both layers are of the SIR type, with the recovery rate being set as $\mu = 1$ for convenience. Initially, a small number of seeds randomly chosen among the permanent residents are placed in both layers. We consider two types of double-layer network configurations: (a) a symmetric configuration with two layers having the same mean degree and (b) an asymmetric configuration in which mean degrees of the two layers differ. The symmetric configuration is idealized and there are no systematic differences between the structures of the two subnetworks, facilitating an understanding of the effects of inter-layer hopping on epidemics. The asymmetric configuration is more realistic, on which we focus our simulations.

3.1. Determination of epidemic threshold

The outbreak threshold is a fundamental quantity in epidemiology. To accurately determine the threshold is thus of considerable interest. A difficulty is that, in the vicinity of the threshold, the outbreak size typically exhibits large fluctuations. A practical approach to accurate numerical determination of the threshold value is through the measure of variability [32] defined as

$$\Delta = \frac{\sqrt{\langle \rho_R^2 \rangle - \langle \rho_R \rangle^2}}{\langle \rho_R \rangle}, \tag{10}$$

where ρ_R is the density of the recovered nodes (i.e., the order parameter), $\langle \rho_R \rangle$ and $\langle \rho_R^2 \rangle$ are the first and second moments of ρ_R, respectively. The variability measure indicates the variation in outbreak sizes over many runs with the same β. In epidemic spreading, the variability typically exhibits a peak in a wide range of values of the infection rate β, the position of which, denoted by β_p^{Δ}, corresponds to the threshold value. Previously, it was shown that the measure is effective for determining the critical points in single layer networks [32]. It is also often used to determine the critical point of phase transition in statistical physics [33].

Here we demonstrate that the variability measure is generally ineffective for determining the threshold of epidemic outbreak in multilayer networks. Fig. 2(a) shows the variability Δ_A of layer A as a function of infection rate β for $m = 0.01$ and $q = 0.1$. We see that Δ_A displays two peaks: at $\beta_p^{\Delta} \approx 0.06$ and 0.1, respectively. Numerically, we find that, in the absence of inter-layer hopping, the isolated threshold value of layer B is $\beta_{Bc}^I \approx 0.05$ for $\langle k_B \rangle = 20$. Thus, for $\beta_B \approx 0.06$, an outbreak will have occurred but there are remarkable fluctuations in the final outbreak size over statistically independent realizations. The fluctuations will propagate to layer A through inter-layer hopping activities, giving rise to the first peak in Fig. 2(a). As the value of the infection rate is increased to $\beta \approx \beta_{Ac}^I = 0.1$, the outbreak of the disease in layer A results in the second peak that is higher than the first one. As we increase the value of q to 0.3, the first peak becomes higher than the second peak. This can be understood by noting that the occurrence of the second peak is the result of the balance of two effects. First, more infected travelers hopping from layer B to layer A will intensify the fluctuations of the final outbreak size in layer A for $\beta \approx 0.06$, as the outbreak in layer B has large fluctuations. But at this infection rate, an outbreak of epidemic does not occur in layer A, as shown in the inset of Fig. 2(a). Second, for $\beta \approx 0.1 > \beta_{Bc}^I$, the outbreak size of layer B is relatively considerable and stable. In fact, a large q value means that more infected travelers will switch from layer B to layer A, reducing the fluctuations in the final outbreak size in layer A. When the value of q is increased to 0.6, the two effects balance out, making the second peak essentially disappear.

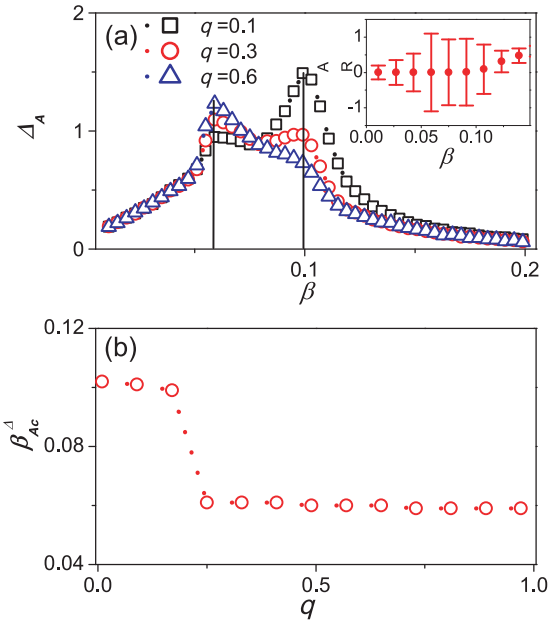

Fig. 2. *Test of whether the variability measure is effective for identifying epidemic thresholds in a given multilayer network.* For a double layer system of random networks with an asymmetric structure, (a) the variability versus the infection rate, and (b) the identified threshold versus the inter-layer hopping rate. Inset in panel (a) shows ρ_R^A values in simulations when $q = 0.3$, and the error bars on the values represent the corresponding variability Δ_A. The parameters are $\langle k_A \rangle = 10$, $\langle k_B \rangle = 20$, and $m = 0.01$, recovery rate $\mu = 1$, each random network layer has $N = N_A = N_B = 10^4$, and all the simulation results are over 5×10^3 dynamical realizations in the same network. As explained in the text, the variability measure for determining the threshold value is not effective for multilayer networks. (For interpretation of the references to color in this figure legend, the reader is referred to the web version of this article.)

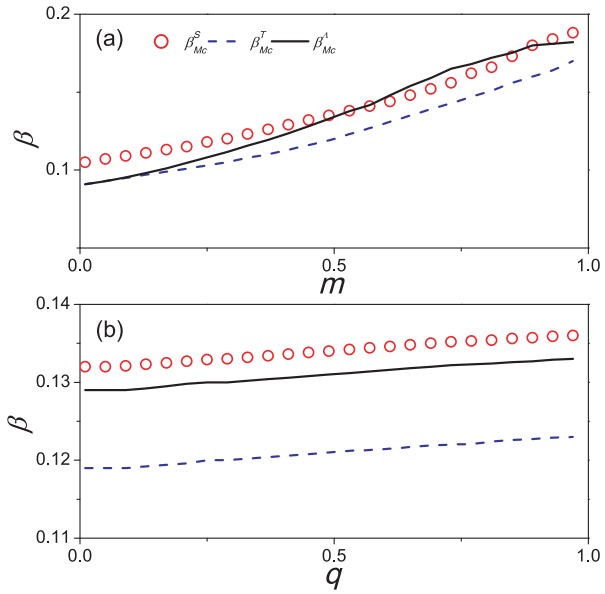

Fig. 3. *Effect of inter-layer hopping on epidemic threshold in a symmetric double layer system of random networks.* Shown is the epidemic threshold versus (a) the fraction m of inter-layer hoppers and (b) the inter-layer switching rate q. The red circles represent the numerically determined values of the threshold β^S_{Mc}, the minimum infection rate with which the final outbreak size ρ_R is equal to or greater than 1%. The blue dash lines are the corresponding, theoretically predicted threshold values (denoted by β^T_{Mc}) from Eqs. (2)–(4), and the black solid lines denote the theoretical thresholds β^{Δ}_{Mc} from the Jacobian matrix in Eqs. (8)-(9). All simulation results are averaged over 10^3 dynamical realizations. In (a), the value of q is fixed at 0.1, and in (b) the value of m is set to be 0.5. Recovery rate is set as $\mu = 1$ in all simulations. (For interpretation of the references to color in this figure legend, the reader is referred to the web version of this article.)

When the threshold value of the outbreak size in layer A has been identified, we can obtain the value of $\beta^{\triangle}_{Ac}$ as a function of q, as shown in Fig. 2(b). It can be seen that the value of $\beta^{\triangle}_{Ac}$ has reduced abruptly from 0.1 to 0.06, which is caused by the infected travelers from layer B. This indicates that the variability measure may not be effective for identifying the epidemic threshold in multilayer networks. In fact, the interplay between the spreading processes in different layers introduces large external fluctuations into the respective dynamics [34], rendering ineffective the variability measure.

In our simulations, we define a reference epidemic threshold to evaluate the outbreak possibility. At the reference threshold, the final outbreak size reaches a pre-specified value (e.g., 0.01) based on a tolerance measure [35,36]. We find that this simple method to be effective for determining the epidemic thresholds in multilayer networks.

3.2. Effect of inter-layer hopping on epidemic dynamics on a double-layer symmetric networked system

To gain preliminary insights, we first study the idealized case of SIR dynamics on a double-layer, symmetric network configuration, where each random network has size $N = N_A = N_B = 10^4$ and mean degree $\langle k_A\rangle = \langle k_B\rangle = 10$. The system symmetry stipulates that the epidemic thresholds for both layers are identical: $\beta^S_{Ac} = \beta^S_{Bc} = \beta^S_{Mc}$, where β^S_{Ac}, β^S_{Bc}, and β^S_{Mc} denote the thresholds of layer A, layer B, and the whole two-layer system, respectively. Fig. 3(a) shows the threshold versus the fraction m of inter-layer travelers for a fixed value of the hopping rate q. We see that the epidemic threshold β^S_{Mc} increases monotonously with m. To gain an understanding of this behavior, we calculate the mean active degree of layer A or layer B. As the hopping leads to holes in each layer, the expected numbers of inter-layer travelers and permanent residents in layers A or B are, respectively, $\langle M_A\rangle = \langle M_B\rangle = 0.5mN$ and $N'_A = N'_B = (1-m)N$. The mean active degree of either layer is thus given by $\langle k'_A\rangle = \langle k'_B\rangle = pN(1-0.5m)$, where p is the connection probability between any pair of nodes in a random network. We have that an increase in m will reduce the mean active degree of both, enhancing the epidemic threshold. Fig. 3(b) shows that an increase in the hopping rate q tends to enhance the epidemic threshold. A larger value of q means that travelers switch between the layers more frequently and are not able to stay in one layer for a relatively long period of time, hindering the spreading process in each layer. We also find that the theoretical thresholds predicted by Eqs. (2)–(4) and the Jacobian matrix in Eqs. (8)–(9) are quite consistent with the numerical results, although the theoretical thresholds are somewhat smaller due to the "echo chamber" effect in the QMF analysis [3].

3.3. Asymmetric double layer system of random networks

We now turn to the general case of asymmetric network configuration: layer A (B) is a sparser (denser) random network with a smaller (larger) mean degree value: $\langle k_A\rangle = 10$ and $\langle k_B\rangle = 20$. The first issue is how inter-layer hopping activities affect

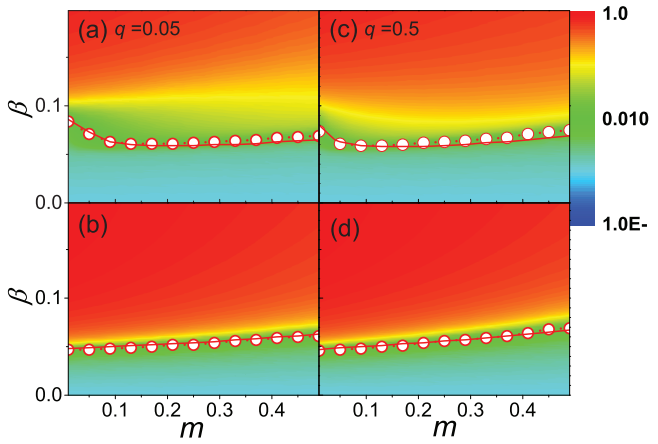

Fig. 4. *Impact of the fraction of inter-layer travelers on the final outbreak size in an asymmetric, double layer system of random networks.* (a,b) For $q = 0.05$, color-coded values of the final outbreak sizes ρ_R^A and ρ_R^B, respectively, in the two-dimensional parameter plane of the infection rate β and the fraction m of the inter-layer travelers. (c,d) The same legends as in (a,b) but for $q = 0.5$. In each panel, the dotted line with red circles represents the thresholds obtained from direct numerical simulations of the SIR dynamics, which is determined as the minimum infection rate β at which the final outbreak size passes through the value of 1%. The red solid curve represents the theoretical thresholds obtained from Eqs. (2)–(4). The sizes of both networks are $N = 10^4$, and each data point in the numerical curve is the result of averaging over 10^3 random realizations of the epidemic dynamics. (For interpretation of the references to color in this figure legend, the reader is referred to the web version of this article.)

the epidemic thresholds in both layers. Fig. 4 shows, for two fixed values of the inter-layer hopping rate q, the dependence of the final outbreak size ρ_R^A (ρ_R^B) of layer A (B) on the infection rate β of the SIR dynamics and on the fraction m of inter-layer travelers. For the sparser layer A, panels (a) and (c) show that the final outbreak size ρ_R^A first increases, reaches a maximum value, and then decreases with m for $\beta \in [0.05, 0.1]$. The epidemic threshold β_{Ac} of the sparser layer displays an analogous non-monotonic behavior. In contrast, for the denser network layer, Fig. 4(b) and (d) show that the value of the outbreak size ρ_R^B decreases monotonously with m, while the epidemic threshold β_{Bc} increases monotonously with m, which are essentially the same qualitative behaviors occurring in the symmetric networks. The theoretically predicted threshold values agree with the simulation results.

The difference between the values of the epidemic threshold in the two layers is shown in Fig. 5. Panels (a) and (c) demonstrate that the threshold β_{Ac}^S of layer A is always smaller than the isolated threshold value β_{Ac}^I in the absence of inter-layer hopping (i.e., without any interaction or coupling with layer B), while the threshold value β_{Bc}^S of layer B is always greater than the value β_{Bc}^I in the absence of any inter-layer hopping activity. These results indicate that the coupling resulting from inter-layer hopping can promote the spreading in the sparser layer but suppress the spreading in the denser layer. A heuristic reason is that, because layer B is more susceptible to an epidemic outbreak than layer A, the number of infected travelers moving from layer B to layer A is in general greater than the number in the opposite direction. As the fraction m of inter-layer travelers is increased [e.g., $m \geq 0.25$ in Fig. 5(a) and $m \geq 0.13$ in Fig. 5(b)], the asymmetric effect becomes more pronounced, making possible nearly simultaneous epidemic outbreak in both layers: $\beta_{Ac}^S \approx \beta_{Bc}^S$. We also observe that increasing the value q of the inter-layer hopping rate enhances the dynamical coupling between the layers, facilitating convergence of the epidemic threshold values of the two layers.

Next we try to understand intuitively the impacts of the fraction of inter-layer travelers on the epidemic threshold and the final outbreak size in each layer. To quantify the asymmetric interplay between the epidemic dynamics on both layers, we define the following deficit of influent infected density:

$$\delta\rho_I = \frac{n_{B\to A}^I - n_{A\to B}^I}{N}, \tag{11}$$

where $n_{B\to A}^I$ is the total number of infected travelers moving from layer B to layer A over the entire spreading process, and $n_{A\to B}^I$ is the number of infected travelers moving in the opposite direction. A positive value of $\delta\rho_I$ means that the inter-layer hopping is beneficial to promoting the spreading process in layer A (or to inhibiting the spreading dynamics in layer B). We see that $\delta\rho_I$ increases with m and reaches its peak at $m \approx 0.13$ for $q = 0.05$ in Fig. 5(b) and $m \approx 0.09$ for $q = 0.5$ in Fig. 5(d). This provides an explanation for the existence of a value of β_{Ac}^S with respect to variations in m at which the outbreak size in the sparser network is maximized. As m and $\delta\rho_I$ increase, inter-layer hopping promotes the spreading process in the sparser layer A, reducing its epidemic threshold. For the m value at which $\delta\rho_I$ reaches its peak value, the promotional effect of inter-layer hopping is maximized. Note that a larger value of m gives a smaller mean active degree of the sparser layer A due to the emergence of more holes, leading to an increase in the epidemic threshold. For the denser layer B with a large mean degree, increasing m always enhances the inhibitory effect of inter-layer hopping on the spreading dynamics, thereby reducing the mean active degree of the network layer and leading to a monotonous increase in the epidemic threshold of the layer.

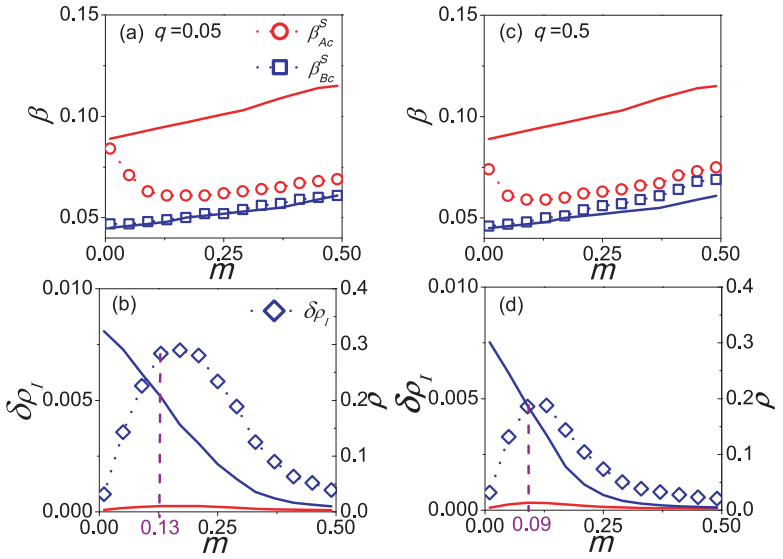

Fig. 5. *The impact of the fraction of inter-layer traveler on the epidemic threshold in an asymmetric, double layer system of random networks.* (a,b) For fixed inter-layer hopping rate $q = 0.05$, epidemic threshold and the deficit of influent infected density versus the fraction m of inter-layer travelers. (c,d) The same legends as for (a,b), respectively, but for $q = 0.5$. In panels (a) and (c), the dotted line with red circles and the dotted line with blue squares, respectively, represents the numerically calculated thresholds β_{Ac}^{S} and β_{Bc}^{S}, and the red solid lines (top) and the blue solid lines (bottom) denote the threshold values β_{Ac}^{I} and β_{Bc}^{I}, respectively, in the absence of inter-layer hopping. In panels (b) and (d), the blue diamonds represent the deficit of the influent infected density $\delta\rho_I$, and the red solid (bottom) and the blue solid (top) curves, respectively, denote the final outbreak sizes ρ_R^A and ρ_R^B of layers A and B. The infection rate of SIR dynamics is set to be $\beta = 0.06$. (For interpretation of the references to color in this figure legend, the reader is referred to the web version of this article.)

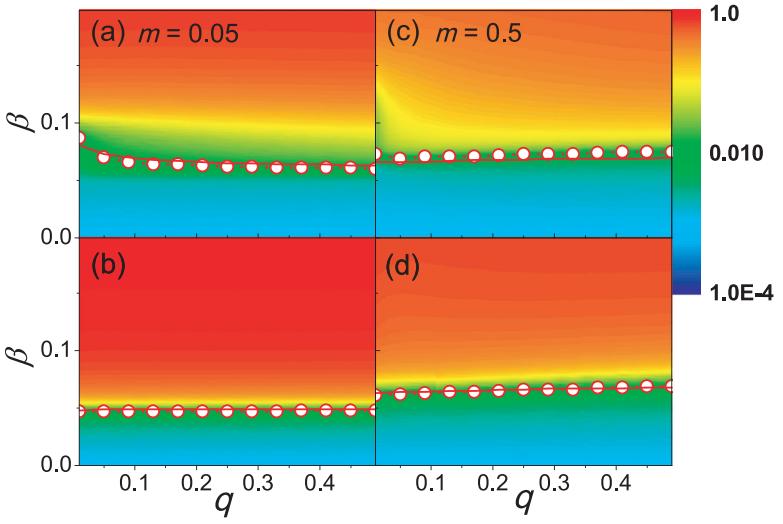

Fig. 6. *Effect of inter-layer hopping rate on the final outbreak size in an asymmetric, double layer system of random networks.* Shown is the final outbreak size ρ_R versus the infection rate β and the inter-layer hopping rate q. (a,b) For $m = 0.05$, variations of ρ_R^A and ρ_R^B, respectively, in the parameter plane (β, q). (c,d) The same legends as in (a,b) but for $m = 0.5$. In each panel, the dotted line with red circles represents the numerically simulated threshold values, which is the minimum value of the infection rate β that satisfies the criterion $\rho_R \geq 0.01$. The red solid curve is the theoretically predicted threshold value from Eqs. (2)-(4). (For interpretation of the references to color in this figure legend, the reader is referred to the web version of this article.)

We now investigate the impacts of varying the inter-layer hopping rate q on the spreading dynamics in both layers. Fig. 6 shows, for two fixed values of m, the dependence of the final outbreak size ρ_R^A (ρ_R^B) of the sparser layer A (the denser layer B) on q and the infection rate β of the SIR process. For a small value of m, ρ_R^A (β_{Ac}) first increases (decreases) with q and then tends to a plateau value, e.g., for $\beta \in [0.05, 0.1]$, as shown in Fig. 6(a). However, ρ_R^B (β_{Bc}) remains approximately constant, e.g., for $\beta \in [0.05, 0.1]$, as shown in Fig. 6(b). For a larger value of m, both ρ_R^A and β_{Ac} versus q display a non-monotonic behavior, e.g., for $\beta \in [0.05, 0.07]$, as shown in Fig. 6(c), but ρ_R^B (β_{Bc}) monotonously decreases (increases) with q, e.g., for $\beta \in [0.05, 0.07]$, as shown in Fig. 6(d). Fig. 7(a) and (c) reveal a a gap between β_{Ac} and β_{Bc} for the case of small m values,

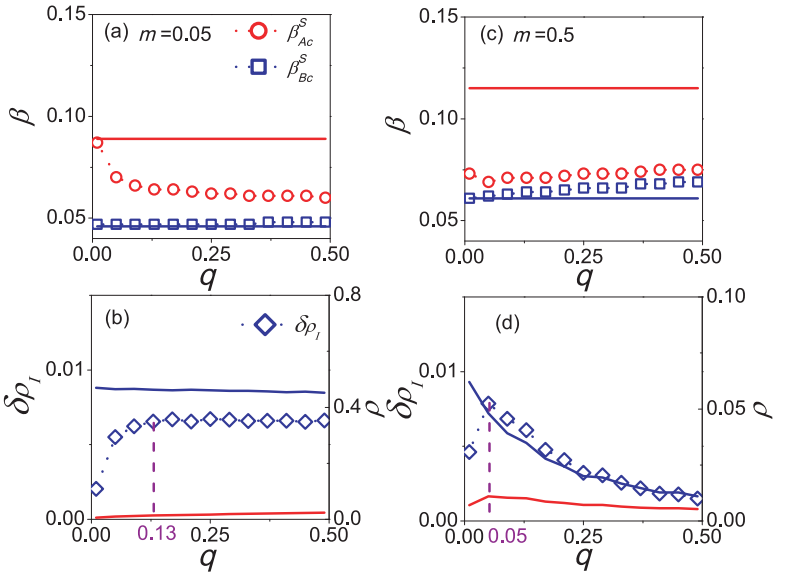

Fig. 7. *Effect of inter-layer hopping rate on epidemic thresholds and outbreak size in an asymmetric, double layer system of random networks.* (a,b) For $m = 0.05$, epidemic threshold and the deficit of influent infected density, respectively, versus the hopping rate q. (c,d) The same plots but for $m = 0.5$. In panels (a) and (c), the dotted line with red circles and dotted line with blues quares, respectively, represents the numerically obtained threshold values β_{Ac}^{S} and β_{Bc}^{S}, and the red solid lines (top) and the blue solid lines (bottom) denote the threshold values β_{Ac}^{I} and β_{Bc}^{I}, respectively, when the dynamics in the two layers are independent of each other in the absence of inter-layer hopping. In panels (b) and (d), the blue diamonds represent the deficit of influent infected density $\delta\rho_I$, and the red solid (bottom) and the blue solid (top) curves, respectively, denote the final outbreak sizes ρ_R^A of layer A and ρ_R^B of layer B. (For interpretation of the references to color in this figure legend, the reader is referred to the web version of this article.)

while a large value of m leads to simultaneous epidemics in both layers. This result indicates that, with respect to changes in the hopping rate q, the variations in the fraction m of inter-layer travelers play a more influential role in determining the dynamical coupling between the layers. As shown in Fig. 7(b), the value of $\delta\rho_I$ increases to a saturated value at $q \approx 0.13$, and so β_{Ac} decreases to a small value, as shown in Fig. 7(a). In Fig. 7(d), for $q > 0.05$, ρ_R^A decreases slowly with q, and the value of $\delta\rho_I$ first increases rapidly and then reaches its peak at $q \approx 0.05$ due to the promoting effect from the dynamics in layer B, causing β_{Ac} to reach a minimum value. In fact, a relatively large value of q means that the travelers switch between layers frequently and so staying on a layer for a long time becomes difficult, hindering the spreading processes on both layers. As a result, ρ_R^B (β_{Bc}) monotonously decreases (increases) with q, especially for large values of m.

3.4. Synthetic and empirical networks

To test the generality of the results on the effects of inter-layer hopping on the epidemic dynamics obtained from the double layer random network model, we carry out simulations on synthetic and empirical networks. Table 1 lists the structural characteristics of the two empirical networks used in our study. In all cases studied, as shown in Fig. 8, the phenomena that the epidemic threshold value β_{Ac} in the sparser layer can be minimum by varying the fraction m of inter-layer travelers and β_{Bc} monotonously increases with m are general. In addition, for the more realistic networks, the phenomenon that a large value of m results in the nearly identical epidemic threshold values in both layers ($\beta_{Ac} \approx \beta_{Bc}$) persists. Representative

Table 1
Topological characteristics of the two empirical networks used in our study. The notations are the following: N is the size of the network layer, $\langle k \rangle$ is the mean degree, k_{min} and k_{max} are the minimum and maximum degrees, respectively, and the degree heterogeneity is calculated from $H = \langle k^2 \rangle / \langle k \rangle^2$. The Wikipedia networks come from the English Wikipedia that describe the voting processes in elections, where the nodes represent individual users and the edges represent the votes. The edges corresponding to the "Support" ("Opposition") votes are assigned to layer A (B). An m fraction of users are randomly chosen as inter-layer travelers. The Email and Blog networks are two alternative social platforms for users, which are integrated into a two-layer network by randomly adding some one-to-one interconnections.

Networks	Layer	Size	$< K >$	K_{min}	K_{max}	H
Wikipedia [37]	Wikipedia Support	7118	10	1	1167	6.62
	Wikipedia Opposition	7118	20	1	1167	5.74
Emails	U. Rovira I virgili emails [38]	1133	9.66	35	71	1.94
	Blogs [39]	1224	38.7	1	5813	3.13

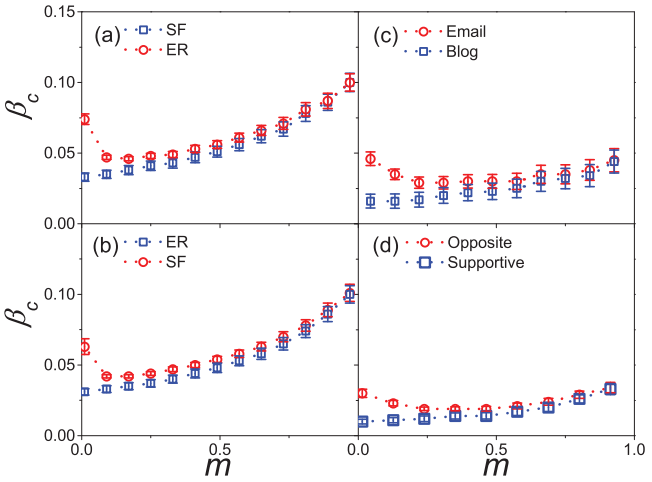

Fig. 8. *The impact of inter-layer hopping on epidemic thresholds of double-layer networks of different topology.* For fixed $q = 0.5$, threshold values β_{Ac}^S and β_{Bc}^S as a function of the fraction m of inter-layer travelers on a synthetic double layer system of (a) sparser random and denser scale-free, (b) sparser scale-free and denser random, (c) Email-Blog networks, and (d) Empirical Wikipedia. The dotted line with red circles and dotted line with blue circles, respectively, stands for β_{Ac}^S and β_{Bc}^S, and the error bars represent the fluctuations of epidemic thresholds over different realizations. In (a), layer A is a random network of average degree $\langle k_A \rangle \approx 10$ while layer B is a scale-free network with algebraic degree exponent $\gamma = 2.0$ and average degree $\langle k_B \rangle \approx 20.6$. In (b), layer A is a scale-free network of degree exponent $\gamma = 2.5$ and average degree $\langle k_A \rangle \approx 3.9$, while layer B is a random network of average degree $\langle k_B \rangle \approx 30$. The size of each network layer is $N = 10^4$. Certain structural characteristics of the two empirical networks in (c) and (d) are listed in Table 1. (For interpretation of the references to color in this figure legend, the reader is referred to the web version of this article.)

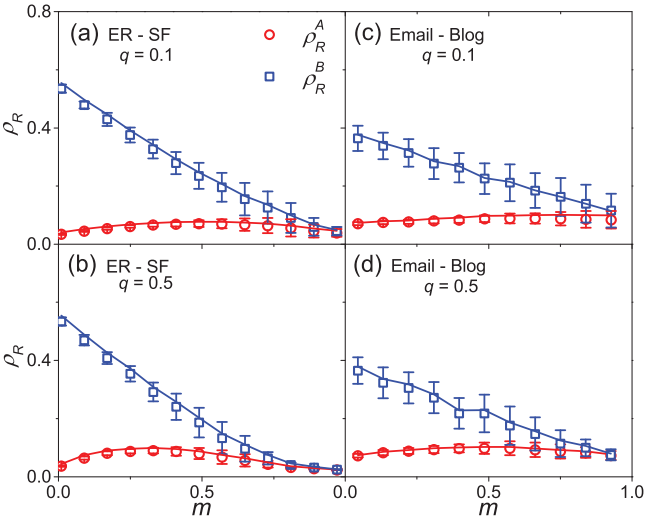

Fig. 9. *Final outbreak size in synthetic and empirical double layer networks.* Shown is the final outbreak size ρ_R versus the fraction m of inter-layer hoppers for a double layer random and Email-Blog networks. (a,b) The results from the double layer random networks for $q = 0.1$ and $q = 0.5$ respectively, for $\beta = 0.07$. (c,d) The results from the Email-Blog double layer system for $q = 0.1$ and $q = 0.5$, respectively, for $\beta = 0.03$. The red circles and blue squares represent the numerically calculated values of the outbreak size ρ_R^A and ρ_R^B, respectively, and the red solid and blue solid curves denote the respective theoretical predictions, and the error bars represent the fluctuations of recovered densities over different realizations. All simulation results are averaged over 5×10^3 dynamical realizations. (For interpretation of the references to color in this figure legend, the reader is referred to the web version of this article.)

behaviors of the final outbreak size for synthetic and empirical double layer systems are shown in Fig. 9. We see that, when the number of inter-layer hoppers becomes significant, the final outbreak sizes on both layers diminish.

3.5. Recurrent epidemics - comparison with real data

Our analysis and numerical results on the epidemic thresholds and final outbreak sizes of asymmetric double-layer systems reveal that inter-layer hopping can promote epidemic spreading in the sparser layer. From the point of view of disease control, this promotional effect is undesired. In general, inter-layer hopping makes the spreading processes more complex with variations, rendering difficult to predict and control the epidemics. Here we wish to point out that our epidemic model

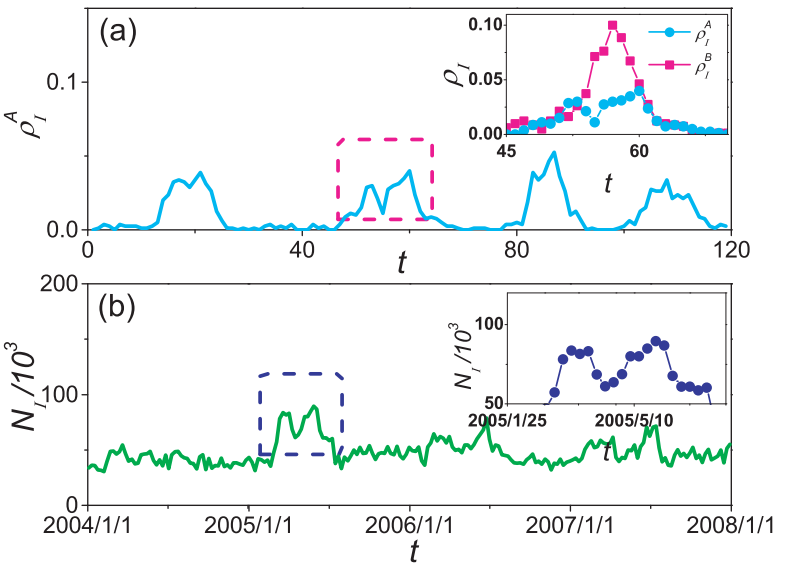

Fig. 10. *Recurrent phenomenon of epidemics on a two-layer network and observed from real data in Hong Kong.* (a) Time evolution of ρ_I^A with four dynamical realizations on a double layer system of random networks, and (b) the empirical time evolution of infectious diseases in Hong Kong. Inset in (a) shows a second (resurgent) outbreak behavior in one realization, and a similar behavior occurs in the real data between 2004 and 2007 in Hong Kong, as shown in the inset of (b). In (a), each network layer size $N = 10^4$, and the average degrees of layers A and B are $\langle k_A \rangle = 10$ and $\langle k_B \rangle = 20$, respectively. Other parameters are $m = 0.4$, $q = 1$, and $\beta = 0.13$. (For interpretation of the references to color in this figure legend, the reader is referred to the web version of this article.)

on multiplex networked systems incorporating inter-layer hopping can exhibit the striking behavior of recurrent or resurgent outbreaks, and we provide a comparison with the behavior extracted from real health data.

We consider the standard setting of a double layer system, each being a random network. Fig. 10(a) shows the time evolution of multiple independent realizations of the SIR spreading dynamics on the sparser layer A. A second wave of epidemics can be seen as shown in the inset, and the second peak is visibly higher than the first one. Using a large number of dynamical realizations, we estimate that the probability for the second outbreak to occur is quite appreciable: $p_{out} = 0.2$, so the perspective that the epidemic can recur certainly cannot be ignored. A heuristic explanation for the recurrent phenomenon is as follows. For $\beta = 0.13$ (slightly greater than the corresponding threshold β_{Ac}^I of layer A in the absence of inter-layer hopping), the seeds in layer-A first infect local neighbors, but the local outbreak is suppressed quickly. Simultaneously, the disease is still raging on in layer B that has denser connections. Travelers may thus bring seeds of epidemic to the unexploited area of layer A, leading to another disease outbreak.

The multiple peaks (or resurgent behavior) of epidemic spreading in multilayer networks have been observed commonly in the real world [40]. For example, Hong Kong Department of Health has organized a surveillance system with the aims to collect empirical data of infectious diseases and to analyze and predict the trend of infection [41]. Weekly consultation rates of influenza-like illness (per 1000 consultations) are collected by the General Practitioners (GP) sentinel system. From the empirical data of the infectious diseases in Hong Kong, we find that a second outbreak with a higher peak occurs in June 2005, as shown in the inset of Fig. 10(b). Our theoretical and computational results provide the following plausible explanation. In March, a disease broke out in Hong Kong and was gradually controlled. But tourists and businessmen from Guangzhou and Macao brought foreign pathogens into Hong Kong, making the disease break out again.

4. Discussion

In complex multilayer networks in the real world, the interactions or coupling among distinct layers can arise from human behaviors. For example, in a social system, nodes and edges can frequently switch between a communication layer and a contact layer. Such switching or hopping behaviors will naturally have effects on the collective dynamics in the network layers involved, but the impacts were not well understood. To fill this knowledge gap, we have articulated a two-layer network model incorporating inter-layer hopping to investigate how it affects the spreading dynamics in both layers. Theoretically, we develop a quenched mean-field method to calculate the two basic quantities underlying any spreading dynamics: the epidemic threshold and the final outbreak size. The framework enables these quantities for both network layers to be predicted. We have carried out extensive numerical simulations on both synthetic and empirical networks, with a focus on the general, asymmetric layer configuration.

Because of the asymmetry, inter-layer hopping can lead to distinct impacts on spreading dynamics in the layers. In particular, for the denser layer, the hopping behavior suppresses the spreading process by enhancing the epidemic threshold.

A large fraction of inter-layer hoppers will induce many “holes” in the denser layer, reducing its active mean degree, and a large hopping rate makes dwelling of the travelers in either layer for a relatively long time difficult. As a result, for the sparser layer, the epidemic threshold exhibits a surprising, non-monotonic behavior with variations in both the fraction of inter-layer travelers and the hopping rate, where the former has a more significant effect on the epidemic dynamics than the latter. As the values of these parameters are increased, the infected travelers will switch from the denser layer to the sparser layer in higher intensity, reducing the epidemic threshold and thus promoting the spreading process in the sparser layer. The subsequent increase in the epidemic threshold in the sparser layer results from similar dynamical effects of inter-layer hopping on the denser layer. As hopping intensifies, the phenomenon of simultaneous breakouts in both layers can occur. Our model predicts another striking phenomenon: recurrence of outbreak. Especially, this can occur on the sparser layer as a result of hopping from the denser layer. The model prediction provides a plausible explanation of the phenomenon of multiple outbreaks in the real world, as supported by data from the epidemics of infectious diseases in Hong Kong.

To incorporate human behaviors into the dynamical processes on multiplex networks is necessary for understanding complex collective dynamics in the real world. Our work represents an attempt in this direction of exciting research. Among many issues, immediate extension of this work could include treating alternative types of spreading dynamics (beyond the SIR type treated in the present work) and studying the impacts of inter-layer hopping on other types of collective dynamics such as synchronization. More human realistic dynamics with heterogeneous interevent time distributions should also be studied [42].

Declaration of Competing Interest

The authors declare that they have no known competing financial interests or personal relationships that could have appeared to influence the work reported in this paper.

CRediT authorship contribution statement

Dayu Wu: Methodology, Investigation, Software, Validation, Formal analysis, Writing - original draft. **Ming Tang:** Conceptualization, Methodology, Formal analysis, Funding acquisition, Writing - review & editing. **Zonghua Liu:** Conceptualization, Resources, Funding acquisition, Supervision. **Ying-Cheng Lai:** Methodology, Funding acquisition, Writing - review & editing.

Acknowledgements

This work was supported by the National Natural Science Foundation of China under Grant Nos. 11975099, 11575041, 11835003, and 11675056, the Natural Science Foundation of Shanghai under Grant No. 18ZR1412200, and the Science and Technology Commission of Shanghai Municipality under Grant No. 14DZ2260800. YCL would like to acknowledge support from the Vannevar Bush Faculty Fellowship program sponsored by the Basic Research Office of the Assistant Secretary of Defense for Research and Engineering and funded by the Office of Naval Research through Grant No. N00014-16-1-2828.

References

[1] Barrat A, Barthélemy M, Vespignani A. Dynamical processes on complex networks. Cambridge, UK: Cambridge University Press; 2008.
[2] Pastor-Satorras R, Castellano C, Van Mieghem P, Vespignani A. Epidemic processes in complex networks. Rev Mod Phys 2015;87(3):925.
[3] Wang W, Tang M, Stanley HE, Braunstein LA. Unification of theoretical approaches for epidemic spreading on complex networks. Rep Prog Phys 2017;80(3):036603.
[4] Wu JT, Leung K, Leung GM. Nowcasting and forecasting the potential domestic and international spread of the 2019-nCoV outbreak originating in Wuhan, China: a modelling study. Lancet 2020.
[5] Gao J, Buldyrev SV, Stanley HE, Havlin S. Networks formed from interdependent networks. Nat Phys 2012;8(1):40–8.
[6] Granell C, Gómez S, Arenas A. Dynamical interplay between awareness and epidemic spreading in multiplex networks. Phys Rev Lett 2013;111(12):128701.
[7] Liu Q-H, Wang W, Cai S-M, Tang M, Lai Y-C. Synergistic interactions promote behavior spreading and alter phase transitions on multiplex networks. Phys Rev E 2018;97:022311. doi:10.1103/PhysRevE.97.022311.
[8] Boccaletti S, Bianconi G, Criado R, Del Genio CI, Gómez-Gardeñes J, Romance M, et al. The structure and dynamics of multilayer networks. Phys Rep 2014;544(1):1–122.
[9] Kivelä M, Arenas A, Barthelemy M, Gleeson JP, Moreno Y, Porter MA. Multilayer networks. J Comp Net 2014;2(3):203–71.
[10] Liu RR, Eisenberg DA, Seager TP, Lai Y-C. The “weak” interdependence of infrastructure systems produces mixed percolation transitions in multilayer networks. Sci Rep 2018;8:2111.
[11] Dickison M, Havlin S, Stanley HE. Epidemics on interconnected networks. Phys Rev E 2012;85(6):066109.
[12] Lee K-M, Brummitt CD, Goh K-I. Threshold cascades with response heterogeneity in multiplex networks. Phys Rev E 2014;90(6):062816.
[13] De Domenico M, Granell C, Porter MA, Arenas A. The physics of spreading processes in multilayer networks. Nat Phys 2016;12(10):901–6.
[14] Saumell-Mendiola A, Serrano MÁ, Boguná M. Epidemic spreading on interconnected networks. Phys Rev E 2012;86(2):026106.
[15] Min B, Gwak S-H, Lee N, Goh K-I. Layer-switching cost and optimality in information spreading on multiplex networks. Sci Rep 2016;6:21392.
[16] Gomez S, Diaz-Guilera A, Gomez-Gardenes J, Perez-Vicente CJ, Moreno Y, Arenas A. Diffusion dynamics on multiplex networks. Phys Rev Lett 2013;110(2):28701.
[17] Asllani M, Busiello DM, Carletti T, Fanelli D, Planchon G. Turing patterns in multiplex networks. Phys Rev E 2014;90(4):42814.
[18] Marceau V, Noël P-A, Hébert-Dufresne L, Allard A, Dubé LJ. Modeling the dynamical interaction between epidemics on overlay networks. Phys Rev E 2011;84(2):026105.
[19] Ruan Z, Tang M, Gu C, Xu J. Epidemic spreading between two coupled subpopulations with inner structures. Chaos 2017;27(10):103104.
[20] De Domenico M, Solé-Ribalta A, Gómez S, Arenas A. Navigability of interconnected networks under random failures. Proc Nat Acad Sci (USA) 2014;111(23):8351–6.

[21] Starnini M, Baronchelli A, Pastor-Satorras R. Effects of temporal correlations in social multiplex networks. Sci Rep 2017;7(1):8597.
[22] Colizza V, Barrat A, Barthélemy M, Vespignani A. The role of the airline transportation network in the prediction and predictability of global epidemics. Proc Nat Acad Sci (USA) 2006;103(7):2015–20.
[23] Volz E. Sir dynamics in random networks with heterogeneous connectivity. J Math Biol 2008;56(3):293–310.
[24] Newman ME. Spread of epidemic disease on networks. Phys Rev E 2002;66(1):016128.
[25] Barthélemy M, Barrat A, Pastor-Satorras R, Vespignani A. Dynamical patterns of epidemic outbreaks in complex heterogeneous networks. J Theo Biol 2005;235(2):275–88.
[26] Miller JC. A note on a paper by Erik Volz: SIR dynamics in random networks. J Math Biol 2011;62(3):349–58.
[27] Valdez LD, Macri PA, Braunstein LA. Temporal percolation of the susceptible network in an epidemic spreading. PloS One 2012;7(9):e44188.
[28] Gómez S, Arenas A, Borge-Holthoefer J, Meloni S, Moreno Y. Discrete-time Markov chain approach to contact-based disease spreading in complex networks. EPL (Europhy Lett) 2010;89(3):38009.
[29] Soriano-Paños D, Lotero L, Arenas A, Gómez-Gardeñes J. Spreading processes in multiplex metapopulations containing different mobility networks. Phys Rev X 2018;8(3):31039.
[30] Van Mieghem P, Omic J, Kooij R. Virus spread in networks. IEEE/ACM Trans Netw (TON) 2009;17(1):1–14.
[31] Shu P, Wang W, Tang M, Zhao P, Zhang Y-C. Recovery rate affects the effective epidemic threshold with synchronous updating. Chaos 2016;26(6):63108.
[32] Shu P, Wang W, Tang M, Do Y. Numerical identification of epidemic thresholds for susceptible-infected-recovered model on finite-size networks. Chaos 2015;25(6):063104.
[33] Yeomans JM. Statistical mechanics of phase transitions. Oxford, UK: Oxford University Press; 1992.
[34] de Menezes MA, Barabási A-L. Separating internal and external dynamics of complex systems. Phys Rev Lett 2004;93(6):068701.
[35] Ferreri L, Bajardi P, Giacobini M, Perazzo S, Venturino E. Interplay of network dynamics and heterogeneity of ties on spreading dynamics. Phys Rev E 2014;90(1):012812.
[36] Liu Q-H, Wang W, Tang M, Zhang H-F. Impacts of complex behavioral responses on asymmetric interacting spreading dynamics in multiplex networks. Sci Rep 2016;6:25617.
[37] Wikipedia elections network dataset – KONECT. 2017a. http://konect.uni-koblenz.de/networks/elec.
[38] U. Rovira i Virgili network dataset – KONECT. 2017b. http://konect.uni-koblenz.de/networks/arenas-email.
[39] Blogs network dataset – KONECT. 2017c. http://konect.uni-koblenz.de/networks/moreno_blogs.
[40] Watts DJ, Muhamad R, Medina DC, Dodds PS. Multiscale, resurgent epidemics in a hierarchical metapopulation model. Proc Nat Acad Sci (USA) 2005;102(32):11157–62.
[41] Zheng Muhua, Wang Chaoqing, Zhou Jie, Zhao Ming, Guan Shuguang, Zou Yong, et al. Non-periodic outbreaks of recurrent epidemics and its network modelling. Scientific Reports 2015;5 In press. doi:10.1038/srep16010.
[42] Holme P, Saramäki J. Temporal networks. Phys Rep 2012;519(3):97–125.